HHS Public Access

Author manuscript

Chem Mater. Author manuscript; available in PMC 2024 November 28.

Published in final edited form as:

Chem Mater. 2023 November 28; 35(22): 9542–9551. doi:10.1021/acs.chemmater.3c01390.

Novel Combination Treatment for Melanoma: FLASH Radiotherapy and Immunotherapy Delivered by a Radiopaque and Radiation Responsive Hydrogel

Yuxi C. Dong,
Department of Radiology, University of Pennsylvania, Philadelphia, Pennsylvania 19104, United States; Department of Bioengineering, University of Pennsylvania, Philadelphia, Pennsylvania 19104, United States

Lenitza M. Nieves,
Department of Biochemistry and Molecular Biophysics, Perelman School of Medicine of the University of Pennsylvania, Philadelphia, Pennsylvania 19104, United States

Jessica C. Hsu,
Department of Radiology, University of Pennsylvania, Philadelphia, Pennsylvania 19104, United States; Department of Bioengineering, University of Pennsylvania, Philadelphia, Pennsylvania 19104, United States

Ananyaa Kumar,
Department of Bioengineering, University of Pennsylvania, Philadelphia, Pennsylvania 19104, United States

Mathilde Bouché,
Université de Lorraine, CNRS, F-54000 Nancy, France

Uma Krishnan,
Department of Radiation Oncology, University of Pennsylvania, Philadelphia, Pennsylvania 19104, United States

Katherine J. Mossburg,
Department of Radiology, University of Pennsylvania, Philadelphia, Pennsylvania 19104, United States; Department of Bioengineering, University of Pennsylvania, Philadelphia, Pennsylvania 19104, United States

Corresponding Authors: **Jay F. Dorsey** – Department of Radiation Oncology, University of Pennsylvania, Philadelphia, Pennsylvania 19104, United States; Jay.Dorsey2@pennmedicine.upenn.edu, **David P. Cormode** – Department of Radiology, University of Pennsylvania, Philadelphia, Pennsylvania 19104, United States; Department of Bioengineering, University of Pennsylvania, Philadelphia, Pennsylvania 19104, United States; David.Cormode@pennmedicine.upenn.edu.

Supporting Information

The Supporting Information is available free of charge at https://pubs.acs.org/doi/10.1021/acs.chemmater.3c01390.
Supporting Information and methods, i.e., materials, synthesis of GSH-coated AuNP, hydrogel characterization, electron microscopies, ICP-OES, EDX, XRD, FT-IR, rheology, hydrogel irradiation, the effect of radiation on AuNP and IMQ release, the effect of oxygen and radical oxygen species (ROS) scavenging on AuNP release, CT phantom imaging, cell culture, ex vivo studies. Supplementary results, i.e., hydrogel characterizations (TEM, SEM, FT-IR, EDX, XRD), effect of radiation dose on AuNP release, rheology, cytokine secretion, viability of cells under various treatments (radiation, IMQ or combinations thereof), histology, body weights, and AuNP biodistribution (PDF)

Complete contact information is available at: https://pubs.acs.org/10.1021/acs.chemmater.3c01390

The authors declare no competing financial interest.

Deeksha Saxena,
Department of Radiation Oncology, University of Pennsylvania, Philadelphia, Pennsylvania 19104, United States

Selen Uman,
Department of Bioengineering, University of Pennsylvania, Philadelphia, Pennsylvania 19104, United States

Taku Kambayashi,
Department of Pathology and Laboratory Medicine, University of Pennsylvania, Philadelphia, Pennsylvania 19104, United States

Jason A. Burdick,
Department of Bioengineering, University of Pennsylvania, Philadelphia, Pennsylvania 19104, United States; Department of Chemical and Biological Engineering, University of Colorado Boulder, Boulder, Colorado 80303, United States

Michele M. Kim,
Department of Radiation Oncology, University of Pennsylvania, Philadelphia, Pennsylvania 19104, United States

Jay F. Dorsey,
Department of Radiation Oncology, University of Pennsylvania, Philadelphia, Pennsylvania 19104, United States

David P. Cormode
Department of Radiology, University of Pennsylvania, Philadelphia, Pennsylvania 19104, United States; Department of Bioengineering, University of Pennsylvania, Philadelphia, Pennsylvania 19104, United States

Abstract

Immunotherapies have become the standard treatment for melanoma. To further improve patient responses, combinations of immunotherapies and radiotherapy (RT) are being studied, since radiotherapies can potentially provide additional immune stimulation, in addition to direct antitumor effects. FLASH-RT is a novel, ultrahigh dose rate, radiation delivery approach, with the potential of at least equivalent tumor control efficacy and reduced damage to healthy tissue. However, the effects of combining FLASH-RT and immunotherapy have not been extensively studied in melanoma. Toll-like receptor (TLR) agonists, such as imiquimod (IMQ), are potent immunostimulatory agents, although their utility is limited due to poor solubility and systemic side effects. We therefore developed a novel combination therapy for melanoma consisting of IMQ delivered to the tumor via a radiopaque and radiation responsive hydrogel combined with FLASH-RT. We found that FLASH was able to effectively stimulate IMQ release from the hydrogel. In addition, we found that the combination of FLASH and released IMQ resulted in synergistic melanoma cell killing *in vitro*. The combination therapy reduced tumor growth compared to controls, enhanced survival, and resulted in remarkable enhancements in certain tumor cytokine levels. CT imaging allowed the hydrogel to be monitored *in vivo*. In addition, no adverse effects of the treatment were observed. Overall, this IMQ-gel and FLASH-RT combination may have

potential as an improved treatment for melanoma and indicates that the interactions of FLASH-RT and TLR agonists merit further study.

Graphical Abstract

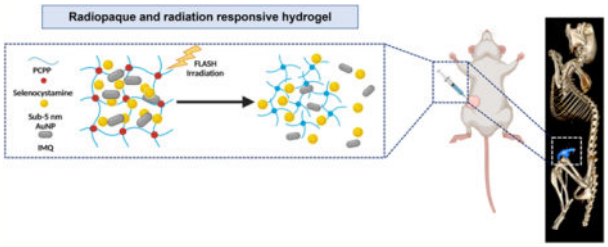

1. INTRODUCTION

Several immunotherapies have been approved by the FDA for use in treating melanoma, such as CTLA-4 inhibitors and PD-1 antibodies. Nevertheless, melanoma is responsible for approximately 71% of skin cancer deaths, over 9,000 each year, largely due to aggressive metastatic disease.[1,2] Therefore, approaches to enhance the effects of immunotherapies are of great interest. Radiotherapies are known to create immunostimulation and changes in the tumor microenvironment, which can result in synergistic effects when combined with immunotherapies.[3] Recently, ultrahigh dose rate radiation, or FLASH-RT, has attracted substantial attention in the radiation oncology field, as it can markedly improve healthy tissue tolerance to radiation damage. FLASH-RT delivers the radiation dose in milliseconds with dose rates exceeding 40 Gy/s, as opposed to conventional radiotherapy, where the same dose is delivered at much slower dose rates (~2 Gy/min) over several weeks for multiple fractions.[4] FLASH-RT can currently be delivered via electron or proton modalities, with the latter much more clinically applicable to deeper-seated tumors. The rationale behind the improved normal tissue tolerance is thought to be the massive oxygen consumption from FLASH-RT, which results in transient protective hypoxia in normal tissue. Despite the promising results being reported for FLASH-RT, the combined effects of FLASH-RT and immunotherapies have received little attention thus far and not at all in melanoma.

IMQ is a TLR 7 agonist used as an immune response modifier that activates the innate immune system. It has been approved by the Food and Drug Administration (FDA) for topical treatment of various skin malignancies and viral warts in the form of a cream that is known as Aldara. IMQ has been studied for its potential use as a treatment for melanoma.[5,6] Interestingly, recent studies have revealed that TLR agonists can activate the host immune system as adjuvants and have emerged as a potential complement to conventional radiotherapy.[7,8] However, the utility of TLR agonists, including IMQ, is limited by their poor solubility that effectively prevents their use as oral drugs as well as undesirable side effects when administered systemically.[9] These limitations have therefore spurred interest in delivery vehicles for TLR agonists that can increase site-specific drug concentrations and reduce systemic exposure to the drug.[10]

In this report, we studied FLASH-RT combined with immunotherapy in the form of a radiation responsive, radiopaque hydrogel loaded with IMQ, as a novel theranostic approach for the treatment of melanoma. The hydrogel used is imageable with CT via inclusion of gold nanoparticles (AuNP) and was previously shown to release an encapsulated drug on demand upon exposure to photon-based radiotherapy.[11] CT is especially valuable in localizing hydrogels *in vivo* since the deployment and retention of the hydrogels can be assessed over time via onboard CT scanners integrated in radiotherapy systems.[12,13] We herein report the formation of this IMQ-loaded hydrogel, its characterization, and its response to exposure to FLASH-RT. We examine the cytocompatibility of the hydrogel and the cytotoxicity and immunostimulatory properties of IMQ released from the hydrogel by FLASH-RT *in vitro*. Moreover, we assess the imaging properties, antitumor effects, immunostimulation, and biocompatibility of the hydrogel/FLASH-RT combination therapy *in vivo*.

2. MATERIALS AND METHODS

2.1. Hydrogel Formation.

2.1.1. AuNP Hydrogel.—The formation of AuNP-hydrogel was adapted from the method previously reported by our group.[11] In brief, 1 mL of PCPP (4 mg mL^{-1}), 5 mg of AuNP solution, and Na_2HPO_4 (10.3 mg, 10.3 mg mL^{-1}, PBS) were mixed together, and HCl (1 M) was added to the mixture to adjust the pH to 7.4. Next, 1.4 μL of selenocystamine dihydrochloride (110 mg mL^{-1}, PBS) was added to the PCPP and AuNP mixture and vortexed for 30 s. The resulting mixture was added into 10 mL of $CaCl_2$ solution (8.8%, DI water) dropwise while stirring at 350 rpm and was left to react for 20 min at room temperature. Following that, the hydrogel was collected and transferred to 15 mL conical tubes and centrifuged at 2,000 rpm for 8 min. The supernatant was discarded, and the hydrogel was resuspended in DI water. This process was repeated three times. Finally, the hydrogel was collected in 1 mL of DI water, centrifuged at 14,000 rpm and stored at 4 °C for subsequent use. The final concentration of AuNP in the sample was determined using ICP-OES.

2.1.2. IMQ-Loaded AuNP Hydrogel.—To load with both hydrogel AuNP and IMQ, 10 μg of IMQ (1 mg mL^{-1}, DMSO) was mixed with the PCPP, AuNP, and Na_2HPO_4 solution described above, and the pH was adjusted to 7.4 by addition of HCl (1 M). The resulting mixture was vortexed and incubated for 10 min before cross-linking with selenocystamine dihydrochloride as described above. The final concentration of IMQ in the sample was determined using UV–visible spectroscopy.

2.2. Cell Culture.

The B16–F10 cell line was used to evaluate the *vitro* biocompatibility of AuNP hydrogel and cytotoxicity of the IMQ released from the IMQ-loaded AuNP hydrogel. Cells were cultured according to the instructions from ATCC at 37 °C and 5% CO_2, and all experiments were performed in triplicate.

2.2.1. Effect of FLASH-RT Combined with Triggered IMQ Release on Cells.—

The IMQ-loaded AuNP hydrogels were prepared as detailed in the Supporting Information. Following the last purification step of IMQ-loaded AUNP hydrogel, an appropriate amount of cell culture media was added to hydrogel based on the AuNP concentration determined through ICP-OES, such that [Au] would be 0.5 mg mL^{-1} if the hydrogel released all of the AuNP. The hydrogels were then irradiated with 0 Gy (mock irradiation), 60 Gy FLASH-RT, or 60 Gy proton irradiation using a conventional dose rate (CONV-RT) before incubating at 37 °C in a water bath for 24 h. Meanwhile, the B16–F10 cells were seeded as detailed in the Supporting Information. Following a 24 h incubation period, the Scells were either treated with 100 μL of IMQ containing supernatants from the hydrogel and then irradiated with 10 Gy FLASH-RT or CONV-RT, or irradiated with 10 Gy FLASH-RT or CONV-RT directly. After the treatments, the cells were further incubated at 37 °C and 5% CO_2 for 48 h. The MTS assay was then performed as described in the Supporting Information.

2.3. Effect of IMQ on Cytokine Secretion.

Proinflammatory cytokines (TNF-α and IL-6) from splenocytes were assessed. Splenocytes were isolated from C57BL/6J mice. To harvest the spleens, mice were euthanized with CO_2 gas followed by cervical dislocation according to the IACUC-approved protocol. The abdominal cavities were opened and then perfused with 20 mL of PBS in the left ventricle. After that, spleens were collected and then transferred to 1 mL of Erythrocyte Lysis Buffer in a 6-well plate. Spleens were mashed using a syringe plunger until the white pulps appeared, and the mashed spleens were incubated with the buffer for 3 min. Spleen mixtures were pipetted slowly onto filter papers placed over 15 mL conical tubes containing 10 mL of DMEM supplemented with FBS buffer, and the resulting cell suspension in media was collected. The mixtures were then centrifuged at 1250 rpm for 5 min. The supernatants were removed, and 1 mL of fresh cell medium was added. The total splenocytes were then plated in 96-well plates using lymphokine-activated killer (LAK) cell medium (α MEM with 10 mM 4-(2-hydroxyethyl)-1-piperazineethanesulfonic acid (HEPES), 1% penicillin-streptomycin-glutamine (PSG), 1×10^{-5} 2-mercaptoethanol, and 10% FBS). After 24 h incubation, the splenocytes were treated with the IMQ released from the IMQ-loaded AuNP hydrogels. The IMQ treatment and FLASH-RT conditions were identical to those described in the Supporting Information. At the end of the treatment, the medium was removed to evaluate the cytokine levels of TNF-α and IL-6 via ELISA kits.

2.4. In Vivo Studies.

All in vivo studies were performed on female C57BL/6J mice that were 12 weeks old. All animal procedures were performed under protocol number 807148, which was approved by the Institutional Animal Care and Use Committee (IACUC) of the University of Pennsylvania. The Public Health Service (PHS) policy on the Humane Care and Use of Laboratory Animals (Public Law 99–158) was followed.

2.4.1. In Vivo B16–F10 Xenograft Melanoma Tumor Model.—

To develop the xenograft B16–F10 tumor model, B16–F10 melanoma cells were cultured as described in previous sections. For inoculation, cells were removed from culture flasks and resuspended in sterile DPBS. Eight $\times 10^4$ cells were subcutaneously implanted on the right flank of mice

and allowed to grow to an average volume of approximately 100 mm^3. Tumor growth and mouse health were monitored daily. Tumor volume was measured with electric calipers every other day and calculated using the following equation: tumor volume = (length × $width^2$)/2. Tumors were allowed to grow up to 1 cm in diameter, as per IACUC standards, after which the mice were sacrificed. For the intratumoral injection, mice were anesthetized with isoflurane, and anesthesia was maintained with isoflurane via the use of a nose cone. Groups received 50 μL of hydrogels ([AuNP] = 8 mg mL^{-1}, [IMQ] = 832 μM) via intratumoral injection on the right flank via the use of a 1 mL syringe and a 25 gauge needle.

2.4.2. In Vivo FLASH-RT.—FLASH-RT was administered to mice 24 h after the hydrogel treatments. The mice were first anesthetized with isoflurane. A total radiation dose of 10 Gy at a dose rate of 95–103 Gy/s was administered using a proton beam with an energy of 230 MeV, delivered via a horizontal beamline in a dedicated research room with an IBA Proteus Plus C230 Cyclotron, through a 1 cm-diameter circular collimator. Mice were placed in the entrance region of the proton depth-dose curve using a shoot-through technique. Additional system setup information and parameters can be found in the Supporting Information.

2.4.3. In Vivo CT Imaging.—*In vivo* CT imaging was performed using a MILabs micro-CT scanner. Mice were scanned before injection, 3 days postinjection, and 14 days postinjection. The following parameters were used to acquire the images: tube voltage = 50 kV, tube current = 190 μA, slice thickness = 100 μm, and in-plane resolution = 100 μm. The obtained images were analyzed using OsirixMD by drawing ROIs in the organs of interest. The ROI segmentation tool was used to delineate the hydrogel from the surrounding[14] tumors. The attenuation values (HU) were recorded.

2.4.4. In Vivo Immune Response Cytokine Profiling Assay.—The immune regulatory effects of IMQ in combination with FLASH-RT were investigated by the Milliplex cytokine/chemokine magnetic bead-based multiplex assay (Millipore Sigma, Burlington, MA). The xenograft B16–F10 tumor model was developed as previously described. Mice were sacrificed at 4 days posttreatment. To prepare the tumor lysates, tumor was collected and weighed, and 10 mL/g of tumor of the Tissue Extract Reagent (Invitrogen, Grand Island, NY) was added. Tumors were homogenized in a homogenizer at 25 Hz for 1 min at 4 °C and centrifuged at 10,000*g* for 5 min at 4 °C. The supernatants were collected, their total protein concentration was measured using Bradford protein assay (Biorad Laboratories, Hercules, CA) and they were diluted to 10 mg protein/mL with 1 × DPBS. The samples were then processed and assayed for cytokine content by the Human Immunology Core at the University of Pennsylvania.

2.4.5. Survival Analysis.—All mice were examined at least twice weekly for distress and body condition, as per IACUC Rodent Tumor and Cancer Model guidelines. Mice were euthanized if the tumor affected their gait or normal posture, ability to eat, urinate, or defecate, independent of the size of the tumor, or if the tumors reached 1 cm in diameter.

The survival time until the mice reached this maximum tumor growth or died was calculated from the date of hydrogel administration (day 0).

2.5. Statistical Analysis.

All *in vitro* experiments were performed independently at least three times. Two-way ANOVA with multiple comparisons was used to examine statistical significance in differences between the groups in all *in vitro* and *in vivo* experiments unless stated otherwise. *P*-values ≤ 0.05 were considered statistically significant. All statistical analyses were carried out using GraphPad Prism 8 software (San Diego, CA).

3. RESULTS

3.1. Synthesis and Characterization of AuNP-IMQ Hydrogel.

The hydrogel fabrication method was adapted and modified from our previous study.[11] AuNP-IMQ-gel consists of a biodegradable polymer PCPP, a radiation-sensitive cross-linker selenocystamine, contrast-generating material sub-5 nm AuNP, and an immunomodulatory drug IMQ (Figure 1). The hydrogel formulation has the ability to load large amounts of cargoes including AuNP and IMQ drugs in a range of concentrations while maintaining the consistency of a hydrogel (Figure S1A,B). To encapsulate the contrast-generating materials and therapeutics, the cargoes were simply added to the polymer solution before the cross-linking process.[11] The dispersion of AuNP in hydrogels was assessed by TEM (Figure S1C). The composition of the AuNP-IMQ-gel was studied with FT-IR (Figure S2A), XRD (Figure S2B), EDX (Figure S2C), and elemental mapping (Figure S3). Scanning electron microscopy (SEM) of the hydrogel revealed a relatively low level of porosity (Figure S4).[15,16]

3.2. FLASH-RT Triggered Hydrogel Degradation.

FLASH-RT delivers radiation dose at a ultrahigh rate, which can reduce radiation-induced normal tissue toxicities.[17,18] To investigate the triggered degradation of the hydrogel by different forms of radiation, the hydrogels were irradiated with photon RT, proton RT at a conventional dose rate (CONV-RT), and proton FLASH-RT. The payloads (i.e., AuNP and IMQ) released from the hydrogels were quantified to confirm the degradation of the hydrogels. Hydrogels irradiated with either photon or proton beams showed significantly higher IMQ release than the nonirradiated hydrogels, suggesting the effectiveness of the radiation-triggered degradation of hydrogels (Figure 1B). However, the payload release upon photon or proton irradiation at conventional dose rates was not different. On the other hand, hydrogels irradiated with FLASH-RT released significantly more IMQ than hydrogels irradiated with photon beams or proton beams at conventional dose rates, indicating that the dose rate of radiation delivery affected the hydrogel degradation. Next, we further investigated the effect of radiation dose on the triggered degradation of hydrogels (Figure 1C), where we found that irradiation with low radiation doses had a moderate effect with both modalities. However, higher radiation doses (i.e., 45 and 60 Gy) proved effective for the triggered release of IMQ. Similarly, the release of AuNP from the hydrogels was quantified with both CONV-RT and FLASH-RT with a range of radiation doses from 0 to 60 Gy. Both modalities had an effect on triggered release of AuNP from hydrogels

(Figure 1D,E), however, FLASH-RT resulted in significantly higher AuNP release rates than CONV-RT (Figure S5).

The mechanical properties of hydrogels with and without FLASH-RT further confirmed the radiation-triggered degradation after FLASH-RT at 60 Gy. Hydrogels that received FLASH-RT had lower storage modulus, loss modulus, and viscosity than hydrogels without RT, due to the degraded cross-links upon the radiation trigger (Figure S6A,B). Both groups showed elastic properties as hydrogels, as indicated by greater storage modulus than loss modulus. Hydrogels showed decreases in viscosity with increasing shear, indicating their shear-thinning properties before and after FLASH-RT (Figure S6C).

Furthermore, the contrast generation of hydrogels, as well as after exposure to FLASH-RT, was examined using a micro-CT system. The X-ray attenuation of the hydrogels is due to loading with a contrast agent, i.e., AuNP, whose strong X-ray attenuation and high density allowed the deployment and retention of the hydrogel to be assessed over time. CT scans demonstrating the ability of micro-CT to distinguish hydrogels irradiated with FLASH-RT are shown in Figure 2A. We observed that there is a significant difference in CT attenuation values between the hydrogel before FLASH-RT and the hydrogel after FLASH-RT, indicating the degradation of hydrogels upon FLASH-RT (Figure 2B). This result supports our assumption that the degradation of the hydrogel can be monitored through CT imaging.

The mechanisms involved in the FLASH-RT-triggered degradation of hydrogels were investigated in an environment in which ROS production is absent. We have previously found the effect of photon radiotherapy on hydrogel degradation to be via ROS generated by irradiation.[11] Diselenium-containing molecules were found to degrade upon radiation-induced ROS response, which is a molecular basis of ionizing radiation.[19] Hydrogels were therefore incubated in degassed medium or in the presence of the well-documented ROS scavenger ascorbic acid (AA), and then treated with FLASH-RT. Significantly less AuNP was released from the hydrogels when incubated in degassed medium or with AA, confirming that FLASH-RT-induced ROS production results in the degradation of the hydrogels (Figure S7B,C).

3.3. In Vitro Cytocompatibility and FLASH-RT Induced Cytotoxicity of AuNP-IMQ-gel.

The high cytocompatibility of AuNP-hydrogel without drug was previously determined with host cells (i.e., hepatocytes (HepG2), kidney cells (Renca), and endothelial cells (SVEC4–10)) in a study from our group.[11] Herein, the cytocompatibility of the AuNP-hydrogel was further assessed on B16–F10 melanoma cells. No acute toxicity was observed with these hydrogels, suggesting the high cytocompatibility of the degradation byproducts from drug-free hydrogels (Figure 3A). Furthermore, we probed the effects of FLASH-RT on B16–F10 melanoma cells. We exposed B16–F10 cells to either FLASH-RT or CONV-RT with a range of radiation doses from 0 to 10 Gy, and the cells were incubated for 48 h before assessing their viability (Figure S8A). Their viability decreased as the radiation dose increased. As can be seen in Figure 3B, no significant difference in cell viability was observed between cells that received FLASH-RT and CONV-RT with the same radiation dose (note that the advantages of FLASH-RT would be observed *in vivo*, as opposed to *in*

vitro). The cytotoxicity of free IMQ on B16–F10 cells was also evaluated (Figure S8B). As expected, higher IMQ concentrations and longer incubation times with cells resulted in more cell killing. The cytotoxicity of enhanced delivery of IMQ by FLASH-RT was evaluated in the same cell line. The combination treatment of FLASH-RT and IMQ resulted in significantly lower cell viability compared to the either treatment alone (Figures 3C and S8C). This result confirmed that the FLASH-RT degradable hydrogel can not only deliver a cytotoxic amount of drug in response to radiation but also has a synergistic effect with cell exposure to FLASH-RT.

3.4. In Vitro Immunostimulation of IMQ and FLASH-RT.

We assessed the cytokine secretion of proinflammatory cytokines, TNF-α and IL-6, upon IMQ treatment to validate that the immunomodulatory properties of IMQ can lead to the upregulation of inflammatory activities. Splenocytes were isolated from mice, and ELISA assays were performed to detect and quantitate the concentration of cytokines. AuNP-IMQ-gel received 60 Gy FLASH-RT and was incubated for 24 h to allow the triggered release of IMQ. We then incubated splenocytes with released IMQ and collected supernatants for ELISA analysis, which revealed a marked increase in both TNF-α and IL-6 levels upon TLR 7 stimulation through IMQ treatment (Figure S7A). This result supports the possibility of increased B16–F10 cell killing via immune cell responses in addition to direct effects.

3.5. Synergistic Antitumor Effect of IMQ Combined with FLASH-RT.

To investigate the anticancer effects of IMQ, FLASH-RT, and the combination of both *in vivo*, we induced xenograft melanoma tumors by subcutaneous implantation of B16–F10 melanoma cells in C57BL/6J mice. Treatment with intratumoral injection of the hydrogel, local irradiation (10 Gy FLASH-RT targeted to the subcutaneous tumor), or the combination of both hydrogel and FLASH-RT started when the tumors were established. The timeline of the study is shown in Figure 4A. AuNP-IMQ-gel and FLASH-RT were compared to four control groups. The survival analysis (log-rank testing) indicated the effectiveness of the treatments. The mice injected with only DPBS all died after 18 days, whereas all mice in the IMQ-gel + FLASH group survived until the end of the study (Figure 4B), which was a statistically significant difference ($p = 0.002$). On the other hand, none of the other groups were statistically significantly different from the DPBS control group.

3.6. In Vivo Cytokine Expression.

Several cytokines have shown their direct antiproliferative activities or indirect stimulation of immune cells against tumor cells.[20] To investigate the potential antitumor activity of cytokines in the FLASH-RT and IMQ combination treatment, a Luminex Multiplex assay was performed to profile the production of cytokines in B16–F10 tumors. Mice received the treatments described in section 3.4. Mice were sacrificed 4 days after FLASH-RT, tumors were collected, and tumor lysates were extracted for cytokine expression analysis. Significant elevations of G-CSF, IL-9, IP-10, MCP-1, MIP-2, and VEGF were observed in groups treated with both FLASH-RT and IMQ, compared to other control groups (Figure 5A,B). A similar pattern of treatment-dependent cytokine expression was observed for other cytokines, such as eotaxin and MIP-1a at much lower concentrations. This potentially

suggests that the synergy of FLASH-RT and IMQ triggered the release of certain cytokines, which may result in antitumor effects.

3.7. CT Monitoring of Hydrogel Degradation.

The *in vivo* degradation of hydrogels can play an important role in achieving the desired therapeutic outcomes. Most radiotherapy systems, including FLASH-RT, use CT for radiation treatment planning, and a radiopaque hydrogel would facilitate precise delivery of radiation treatments and hydrogel monitoring over time.[13,21] Moreover, imaging the hydrogel can provide insight into the release kinetics of payloads. Therefore, to confirm the radiopacity and imageable properties of hydrogels *in vivo*, we used CT imaging to track the erosion of hydrogel over time. Mice were scanned with a micro-CT system before the hydrogel administration and at 3 and 14 days after the injection. Representative 2D and 3D images from a mouse injected with AuNP-IMQ hydrogel and treated with FLASH-RT are shown in Figure 6A,B. Hydrogels in the tumor tissues were visualized and delineated due to the production of strong CT contrast by AuNP. The ROI of the injection site was isolated and highlighted in both 2D and 3D images (Figure 6C). The volume of the hydrogels was found to be significantly lower in the IMQ-gel + FLASH group versus the IMQ-gel group at 14 days after the hydrogel administration (Figure 6D). The results confirmed the enhanced degradability of hydrogels with FLASH-RT and their *in vivo* biodegradability over time.

3.8. In Vivo Histopathological Analysis and Biodistribution of Released AuNP.

As shown in Figure S9, H&E staining of the major organs did not reveal any noticeable changes in the tissue structures of both control (DPBS) and hydrogel-treated groups, confirming that there are no acute toxicity or adverse effects and supporting the *in vivo* tolerability of the hydrogels. On the other hand, tumor necrosis was observed in hydrogel and FLASH-RT-treated mice, indicating the death of portions of tumor cells after the treatments. No significant difference in the weight of mice in any treatment group was observed (Figure S10) and no adverse effects were observed, suggesting the high tolerability of the hydrogels to mice.

Furthermore, we investigated the biodistribution of the released AuNP from the hydrogel. The key to potential translation of nanoparticle contrast agents is efficient renal clearance so that the toxicity concerns that arise from long-term retention in the reticuloendothelial system (RES) can be avoided. We used sub-5 nm AuNP as the contrast-generating material in the hydrogels since they are known for their excellent excretion profile and low retention in the body.[22] The total gold content in major organs was found to be 4.0% ID, suggesting a low AuNP retention (Figure S11). On the other hand, 49% ID of AuNP was found in tumors, which was expected since a fraction of hydrogel had not degraded at the time mice were sacrificed for analyses. From our previous study with this hydrogel, excretion of the AuNP at longer time points (i.e., 100 days postadministration) is expected to be much closer to 100%.[11]

4. DISCUSSION

In this study, we have developed a combination therapy for treatment of melanoma by combining the novel radiation responsive AuNP-IMQ-gel and FLASH-RT. The radiation sensitivity of the AuNP-IMQ-gel allows for the FLASH-triggered release of IMQ as part of the combination therapy. FLASH-RT has been extensively studied over the past few years since the treatment of the first patient with FLASH-RT in Switzerland.[4] However, most research has been focusing on the physics, biological mechanisms, and their advantages over traditional radiotherapies.[23] In fact, this is the first study that uses FLASH-RT to assist drug delivery with a hydrogel and combines FLASH-RT and immunotherapy to treat melanoma. Our *in vitro* drug release and *in vivo* mice tumor study results indicate that this hydrogel formulation is not only sensitive to photon RT but also to FLASH-RT. There has been a significant amount of research reported on hydrogels with stimuli-responsive properties where external triggers such as temperature, pH, light, and magnetic and electric fields are developed.[24–27] However, using radiation, especially FLASH-RT, as an external stimulus to regulate the hydrogel network degradation to control the release of drug molecules has multiple benefits over the other aforementioned triggers. First, our approach is efficient, as FLASH-RT plays two roles: as an anticancer treatment and as a trigger for drug release, so that no additional external stimuli need to be introduced. Second, FLASH-RT can be easily externally administered on demand with, in effect, no depth penetration limit.[28]

To demonstrate the synergistic anticancer effects of the immunotherapy drug and RT, we combined the AuNP-IMQ-gel and FLASH-RT treatments on a B16–F10 melanoma mouse model. This combination treatment resulted in markedly greater anticancer activity both *in vitro* and *in vivo* than either AuNP-IMQ-gel or FLASH-RT monotherapy, suggesting that FLASH-RT is a potent adjuvant to IMQ delivered by hydrogel. Our findings agree with the results of a combined IMQ and RT study reported by Cho et al., although they used conventional photon RT instead of FLASH-RT and subcutaneous IMQ injections.[29] Their study showed that IMQ not only promotes autophagic cell death *in vitro* but also enhances anticancer immunity in an *in vivo* melanoma mouse model, suggesting that IMQ could be used as a synergistic adjuvant to cancer radiotherapy for melanoma patients.[29] Moreover, our remarkable finding with *in vivo* chemokine and cytokine release showed the local activities of effector T cells. In particular, the elevated IP-10 level indicated that $CD8^+$ T cells were recruited during the combination treatment as studies have shown the crucial role for the chemokine CXCL10 in the recruitment of effector $CD8^+$ T cells.[30] In addition, the boosting effect of antitumor immunity is not limited to IMQ; other TLR 7/8 agonists such as 3M-011 have also been studied for their potential to augment immune response when combined with RT.[31] TLR4-dependent contribution of the immune system to radiotherapy has also been investigated.[32] In fact, there has been evidence that radiotherapy may activate effectors of innate immunity through TLR-dependent mechanisms, thereby augmenting the adaptive immune response to cancer.[33] Overall, radiotherapy has the potential to be an important adjunct to immunotherapies. However, more immune-mediated mechanisms need to be investigated to better understand this combination therapy, especially with FLASH-RT.

The radioactivity of hydrogels was enabled by the loading of AuNP contrast agents. The *in vivo* degradation of hydrogels was monitored and quantified using a CT system. Radiopaque

hydrogels are most often used as radiopaque markers, known as fiducials, to assist local therapy targeting and radiographic tumor and normal tissue localization.[34–36] Alternatively, they can be used in wound healing, for instance, to prevent postoperative adhesions, or in tissue engineering to evaluate the formation of new tissues.[37–39] However, few studies have used radiopaque hydrogels for drug delivery to date.[40–42] Thus, our study presents the potential use of CT imaging in drug delivery using hydrogels.

While signs of the effectiveness of combination therapy of AuNP-IMQ hydrogel and FLASH-RT have been indicated in this study, we recognize some of the limitations of this study and thus more extensive investigations will need to be performed. For example, the safety of the hydrogel studied here is limited to the B16–F10 cell line and mouse model, and longer-term studies of its biocompatibility and *in vivo* toxicology are desired for further clinical translation. For the animal study, we studied only female mice. Since gender differences could lead to different efficacy outcomes, a comparison between the genders would be an important point for future studies. The most effective drug dose regimens can be further identified and optimized by performing additional antitumor control studies. In addition, an examination of hydrogel degradation at multiple time points for longer durations in animal models would be needed to fully understand the long-term degradation profile of the hydrogel. Comparisons of the in vivo therapeutic effects of the hydrogel in combination with FLASH-RT and conventional radiotherapies should be done. Lastly, studying systemic antitumor immune activity upon the combination treatment would further help to improve our understanding of the mechanisms of these antitumor effects.

5. CONCLUSIONS

In this study, we reported a combination therapy using AuNP-IMQ-gel and FLASH-RT that effectively suppressed tumor growth in a mouse model of B16–F10 melanoma. The injectable, radiopaque AuNP-IMQ-gel releases the immunomodulatory and tumor cell killing TLR 7 agonist IMQ upon a FLASH-RT trigger. For the first time, proton FLASH-RT was used in a drug delivery application, and its effectiveness for tumor control and immunostimulation was shown. We found that the combination therapy has significantly higher anticancer effect compared to both AuNP-IMQ-gel or FLASH-RT alone, suggesting that our AuNP-IMQ-gel can be an effective adjuvant candidate to FLASH-RT for the treatment of radioresistant melanoma. In addition, our histopathological investigations confirmed the tolerability of hydrogels within our study time frame. Moreover, *in vivo* CT imaging results confirmed the strong CT contrast generation provided by the AuNP payload in the hydrogel, suggesting the potential of long-term *in vivo* monitoring of residence time and degradation of hydrogel over time. Overall, our findings demonstrate that the AuNP-IMQ-gel and FLASH-RT combination therapy is a promising treatment method for melanoma and that the combination of FLASH-RT and the TLR agonist merits further study.

Supplementary Material

Refer to Web version on PubMed Central for supplementary material.

ACKNOWLEDGMENTS

This work was supported by funding from a UPenn Radiation Oncology Translational Center of Excellence pilot grant, to D.P.C. and J.F.D., the National Institutes of Health (R01 – CA227142-02S1 to L.M.N.), and a Brody Family Medical Trust Fund Fellowship to J.C.H. The content is solely the responsibility of the authors and does not necessarily represent the official views of the NIH. We thank Eric Blankemeyer from the University of Pennsylvania for his help with micro-CT scans, and Biao Zuo for support with the TEM micrographs. This work was carried out in part at the Singh Center for Nanotechnology, part of the National Nanotechnology Coordinated Infrastructure Program.

Data Availability Statement

The data sets generated during and/or analyzed during the current study are available from the corresponding author upon reasonable request.

REFERENCES

(1). Prescott LS; Papadopoulos NE; Euscher ED; Watkins JL; Schmeler KM Topical treatment of recurrent vaginal melanoma in situ with imiquimod: A case report. Gynecol. Oncol. Case Rep 2012, 2 (3), 92–93. [PubMed: 24371630]

(2). Shain AH; Bastian BC From melanocytes to melanomas. Nat. Rev. Cancer 2016, 16 (6), 345–358. [PubMed: 27125352]

(3). Lancellotta V; Del Regno L; Di Stefani A; Fionda B; Marazzi F; Rossi E; Balducci M; Pampena R; Morganti AG; Mangoni M; et al. The role of stereotactic radiotherapy in addition to immunotherapy in the management of melanoma brain metastases: results of a systematic review. Radiol. Med 2022, 127 (7), 773–783. [PubMed: 35606609]

(4). Bourhis J; Sozzi WJ; Jorge PG; Gaide O; Bailat C; Duclos F; Patin D; Ozsahin M; Bochud F; Germond JF; et al. Treatment of a first patient with FLASH-radiotherapy. Radiother. Oncol 2019, 139, 18–22. [PubMed: 31303340]

(5). Kang HY; Park TJ; Jin SH Imiquimod, a Toll-like receptor 7 agonist, inhibits melanogenesis and proliferation of human melanocytes. J. Invest. Dermatol 2009, 129 (1), 243–246. [PubMed: 18596825]

(6). Huang S-W; Wang S-T; Chang S-H; Chuang K-C; Wang H-Y; Kao J-K; Liang S-M; Wu C-Y; Kao S-H; Chen Y-J; Shieh JJ Imiquimod Exerts Antitumor Effects by Inducing Immunogenic Cell Death and Is Enhanced by the Glycolytic Inhibitor 2-Deoxyglucose. J. Invest. Dermatol 2020, 140 (9), 1771–1783.E6. [PubMed: 32035924]

(7). Marabelle A; Filatenkov A; Sagiv-Barfi I; Kohrt H Radiotherapy and toll-like receptor agonists. Semin. Radiat. Oncol 2015, 25 (1), 34–39. [PubMed: 25481264]

(8). Demaria S; Bhardwaj N; McBride WH; Formenti SC Combining radiotherapy and immunotherapy: a revived partnership. Int. J. Radiat. Oncol. Biol. Phys 2005, 63 (3), 655–666. [PubMed: 16199306]

(9). Savjani KT; Gajjar AK; Savjani JK Drug Solubility: Importance and Enhancement Techniques. ISRN Pharm. 2012, 2012, No. 195727. [PubMed: 22830056]

(10). Varshney D; Qiu SY; Graf TP; McHugh KJ Employing Drug Delivery Strategies to Overcome Challenges Using TLR7/8 Agonists for Cancer Immunotherapy. AAPS J. 2021, 23 (4), 90. [PubMed: 34181117]

(11). Bouché M; Dong YC; Sheikh S; Taing K; Saxena D; Hsu JC; Chen MH; Salinas RD; Song H; Burdick JA; et al. Novel treatment for glioblastoma delivered by a radiation responsive and radiopaque hydrogel. ACS Biomater. Sci. Eng 2021, 7 (7), 3209–3220. [PubMed: 34160196]

(12). Davis AT; Palmer AL; Nisbet A. Can. CT scan protocols used for radiotherapy treatment planning be adjusted to optimize image quality and patient dose? A systematic review. British J. Radiol 2017, 90 (1076), 20160406.

(13). Maxim PG; Tantawi SG; Loo BW PHASER: A platform for clinical translation of FLASH cancer radiotherapy. Radiother. Oncol 2019, 139, 28–33. [PubMed: 31178058]

(14). Garrett R; Niiyama E; Kotsuchibashi Y; Uto K; Ebara M Biodegradable Nanofiber for Delivery of Immunomodulating Agent in the Treatment of Basal Cell Carcinoma. Fibers 2015, 3, 478–490.

(15). Přádný M; louf M; Martinová L; Michálek J Macroporous hydrogels based on 2-hydroxyethyl methacrylate. Part 7: Methods of preparation and comparison of resulting physical properties. e-Polym. 2010, 10, 043.

(16). Suneetha M; Rao KM; Han SS Mussel-Inspired Cell/Tissue-Adhesive, Hemostatic Hydrogels for Tissue Engineering Applications. ACS Omega 2019, 4 (7), 12647–12656. [PubMed: 31460385]

(17). Baumann BC; Mitra N; Harton JG; Xiao Y; Wojcieszynski AP; Gabriel PE; Zhong H; Geng H; Doucette A; Wei J; et al. Comparative Effectiveness of Proton vs Photon Therapy as Part of Concurrent Chemoradiotherapy for Locally Advanced Cancer. JAMA Oncol. 2020, 6 (2), 237–246. [PubMed: 31876914]

(18). Schulz-Ertner D; Tsujii H Particle radiation therapy using proton and heavier ion beams. J. Clin. Oncol 2007, 25 (8), 953–964. [PubMed: 17350944]

(19). Zhou G Mechanisms underlying FLASH radiotherapy, a novel way to enlarge the differential responses to ionizing radiation between normal and tumor tissues. Radiat. Med. Protection 2020, 1 (1), 35–40.

(20). Berraondo P; Sanmamed MF; Ochoa MC; Etxeberria I; Aznar MA; Pérez-Gracia JL; Rodríguez-Ruiz ME; Ponz-Sarvise M; Castañón E; Melero I Cytokines in clinical cancer immunotherapy. Br. J. Cancer 2019, 120 (1), 6–15. [PubMed: 30413827]

(21). van Elmpt W; Landry G; Das M; Verhaegen F Dual energy CT in radiotherapy: Current applications and future outlook. Radiother. Oncol 2016, 119 (1), 137–144. [PubMed: 26975241]

(22). Hirn S; Semmler-Behnke M; Schleh C; Wenk A; Lipka J; Schäffler M; Takenaka S; Möller W; Schmid G; Simon U; Kreyling WG Particle size-dependent and surface charge-dependent biodistribution of gold nanoparticles after intravenous administration. Eur. J. Pharm. Biopharm 2011, 77 (3), 407–416. [PubMed: 21195759]

(23). Durante M; Bräuer-Krisch E; Hill M Faster and safer? FLASH ultra-high dose rate in radiotherapy. Br. J. Radiol 2017, 91 (1082), No. 20170628.

(24). Huang H; Qi X; Chen Y; Wu Z Thermo-sensitive hydrogels for delivering biotherapeutic molecules: A review. Saudi Pharm. J 2019, 27 (7), 990–999. [PubMed: 31997906]

(25). Rizwan M; Yahya R; Hassan A; Yar M; Azzahari AD; Selvanathan V; Sonsudin F; Abouloula CN pH Sensitive Hydrogels in Drug Delivery: Brief History, Properties, Swelling, and Release Mechanism, Material Selection and Applications. Polymers 2017, 9 (4), 137. [PubMed: 30970818]

(26). Li L; Scheiger JM; Levkin PA Design and Applications of Photoresponsive Hydrogels. Adv. Mater 2019, 31 (26), No. 1807333.

(27). Liu Z; Liu J; Cui X; Wang X; Zhang L; Tang P Recent Advances on Magnetic Sensitive Hydrogels in Tissue Engineering. Front. Chem 2020, 8, 124. [PubMed: 32211375]

(28). Lin X; Wang X; Zeng L; Wu ZL; Guo H; Hourdet D Stimuli-Responsive Toughening of Hydrogels. Chem. Mater 2021, 33 (19), 7633–7656.

(29). Cho JH; Lee HJ; Ko HJ; Yoon BI; Choe J; Kim KC; Hahn TW; Han JA; Choi SS; Jung YM; et al. The TLR7 agonist imiquimod induces anti-cancer effects via autophagic cell death and enhances anti-tumoral and systemic immunity during radiotherapy for melanoma. Oncotarget 2017, 8 (15), 24932–24948. [PubMed: 28212561]

(30). Reschke R; Yu J; Flood BA; Higgs EF; Hatogai K; Gajewski TF Immune cell and tumor cell-derived CXCL10 is indicative of immunotherapy response in metastatic melanoma. J. ImmunoTherapy Cancer 2021, 9 (9), No. e003521.

(31). Schölch S; Rauber C; Tietz A; Rahbari NN; Bork U; Schmidt T; Kahlert C; Haberkorn U; Tomai MA; Lipson KE; et al. Radiotherapy combined with TLR7/8 activation induces strong immune responses against gastrointestinal tumors. Oncotarget 2015, 6 (7), 4663–4676. [PubMed: 25609199]

(32). Apetoh L; Ghiringhelli F; Tesniere A; Obeid M; Ortiz C; Criollo A; Mignot G; Maiuri MC; Ullrich E; Saulnier P; et al. Toll-like receptor 4–dependent contribution of the immune system

to anticancer chemotherapy and radiotherapy. Nat. Med 2007, 13 (9), 1050–1059. [PubMed: 17704786]

(33). Roses RE; Xu M; Koski GK; Czerniecki BJ Radiation therapy and Toll-like receptor signaling: implications for the treatment of cancer. Oncogene 2008, 27 (2), 200–207. [PubMed: 18176601]

(34). de Souza Lawrence L; Ford E; Gilbert C; Yarmus L; Meneshian A; Feller-Kopman D; Hales R Novel Applications of an Injectable Radiopaque Hydrogel Tissue Marker for Management of Thoracic Malignancies. Chest 2013, 143 (6), 1635–1641. [PubMed: 23287908]

(35). Bair RJ; Bair E; Viswanathan AN A radiopaque polymer hydrogel used as a fiducial marker in gynecologic-cancer patients receiving brachytherapy. Brachytherapy 2015, 14 (6), 876–880. [PubMed: 26481393]

(36). Struik GM; Hoekstra N; Klem TM; Ghandi A; Verduijn GM; Swaak-Kragten AT; Schoonbeek A; de Vries KC; Sattler MA; Verhoef K; et al. Injection of radiopaque hydrogel at time of lumpectomy improves the target definition for adjuvant radiotherapy. Radiother. Oncol 2019, 131, 8–13. [PubMed: 30773191]

(37). Lei K; Chen Y; Wang J; Peng X; Yu L; Ding J Noninvasive monitoring of in vivo degradation of a radiopaque thermoreversible hydrogel and its efficacy in preventing postoperative adhesions. Acta Biomater. 2017, 55, 396–409. [PubMed: 28363786]

(38). Datta S; Jana S; Das A; Chakraborty A; Chowdhury AR; Datta P Bioprinting of radiopaque constructs for tissue engineering and understanding degradation behavior by use of Micro-CT. Bioactive Mater. 2020, 5 (3), 569–576.

(39). Celikkin N; Mastrogiacomo S; Walboomers XF; Swieszkowski W Enhancing X-ray Attenuation of 3D Printed Gelatin Methacrylate (GelMA) Hydrogels Utilizing Gold Nanoparticles for Bone Tissue Engineering Applications. Polymers 2019, 11 (2), 367. [PubMed: 30960351]

(40). Dong YC; Bouché M; Uman S; Burdick JA; Cormode DP Detecting and Monitoring Hydrogels with Medical Imaging. ACS Biomater. Sci. Eng 2021, 7 (9), 4027–4047. [PubMed: 33979137]

(41). Rossi SM; Murray TE; Cassidy J; Lee MJ; Kelly HM A Custom Radiopaque Thermoresponsive Chemotherapy-Loaded Hydrogel for Intratumoural Injection: An In Vitro and Ex Vivo Assessment of Imaging Characteristics and Material Properties. Cardiovasc. Interventional Radiolo 2019, 42, 289–297.

(42). Keshavarz M; Moloudi K; Paydar R; Abed Z; Beik J; Ghaznavi H; Shakeri-Zadeh A Alginate hydrogel co-loaded with cisplatin and gold nanoparticles for computed tomography image-guided chemotherapy. J. Biomater. Appl 2018, 33 (2), 161–169. [PubMed: 29933708]

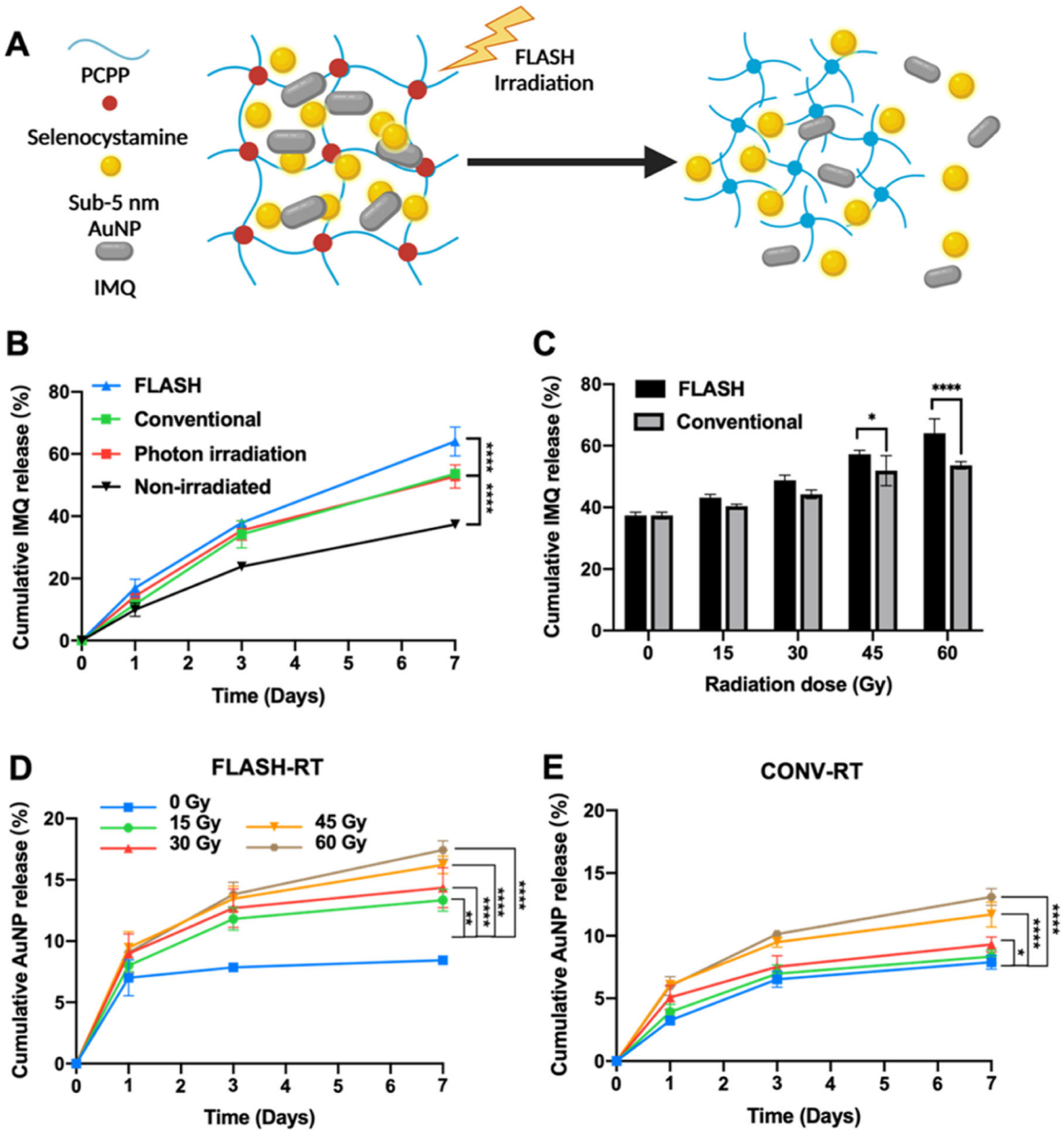

Figure 1.

(A) Schematic representation of the FLASH-RT triggered release of IMQ drug and AuNP from the AuNP-IMQ hydrogel. Influence of radiation on the release of payloads from hydrogels. Quantification of the released IMQ from the hydrogel irradiated with (B) FLASH-RT of 60 Gy, CONV-RT of 60 Gy, photon radiation of 60 Gy, or mock irradiation of 0 Gy. (C) FLASH-RT and CONV-RT with radiation dose from 0 to 60 Gy. Quantification of the released gold from the hydrogel irradiated with (D) FLASH-RT (E) CONV-RT with radiation dose from 0 to 60 Gy.

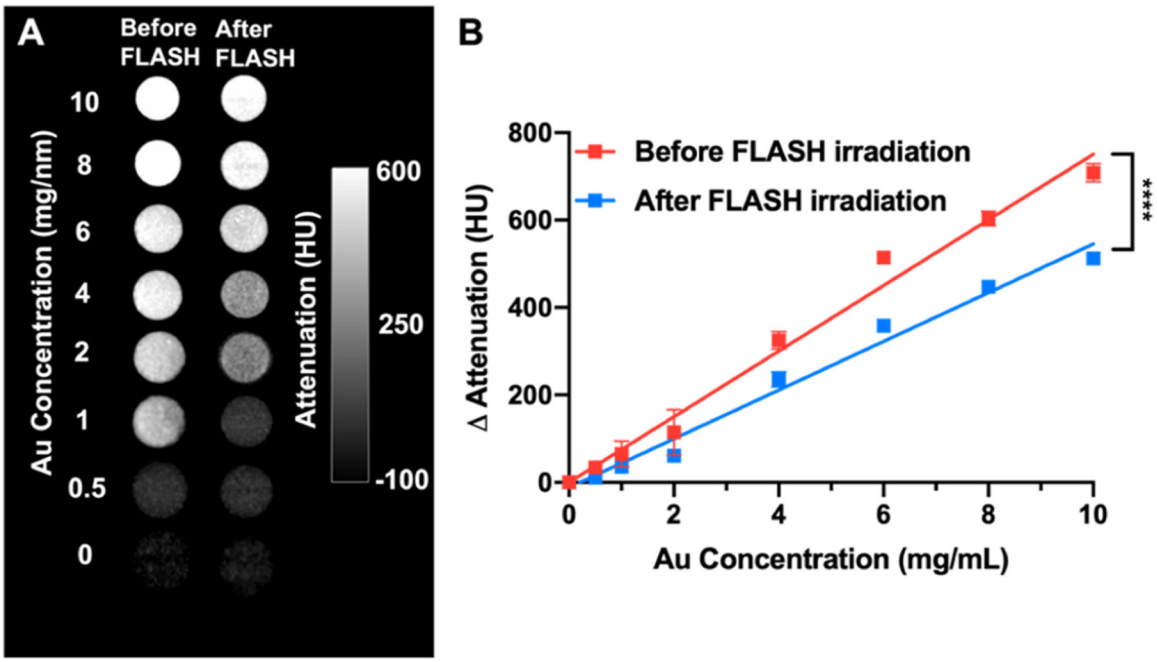

Figure 2.

Phantom imaging of hydrogels with a micro-CT. (A) CT phantom scans of hydrogels before and 7 days after FLASH-RT. (B) Quantification of CT attenuation values of the images in panel (A).

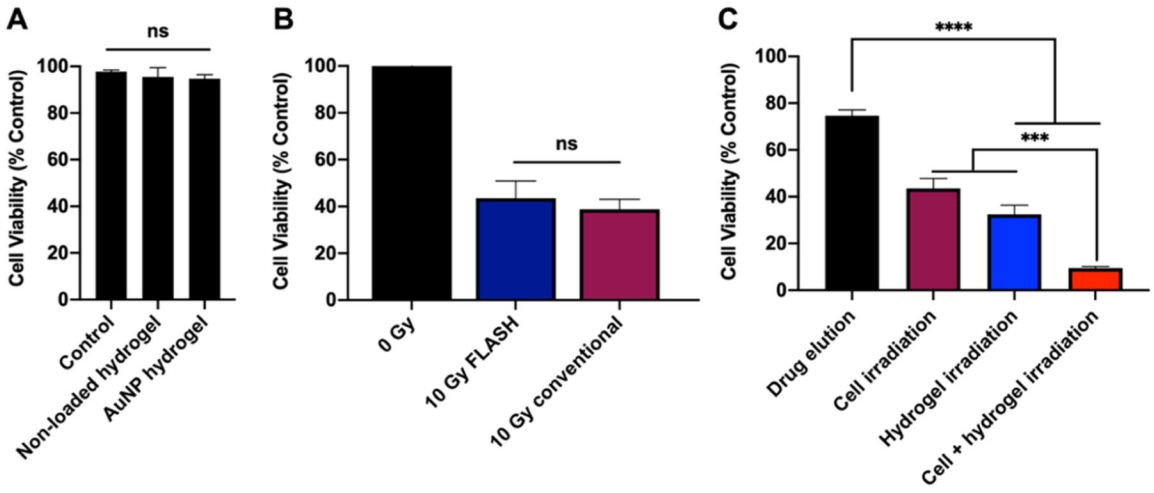

Figure 3.

(A) Effect of AuNP-IMQ-gel on B16–F10 cell viability after 8 h incubation. (B) Effect of 10 Gy FLASH-RT and 10 Gy CONV-RT on B16–F10 cell viability after 48 h incubation. (C) Viability of B16–F10 cells after receiving treatment of eluted drug from the nonirradiated AuNP-IMQ-gel, 10 Gy FLASH-RT, FLASH-triggered released drug from AuNP-IMQ-gel, or the combination of FLASH-RT and FLASH-triggered released drug from AuNP-IMQ-gel.

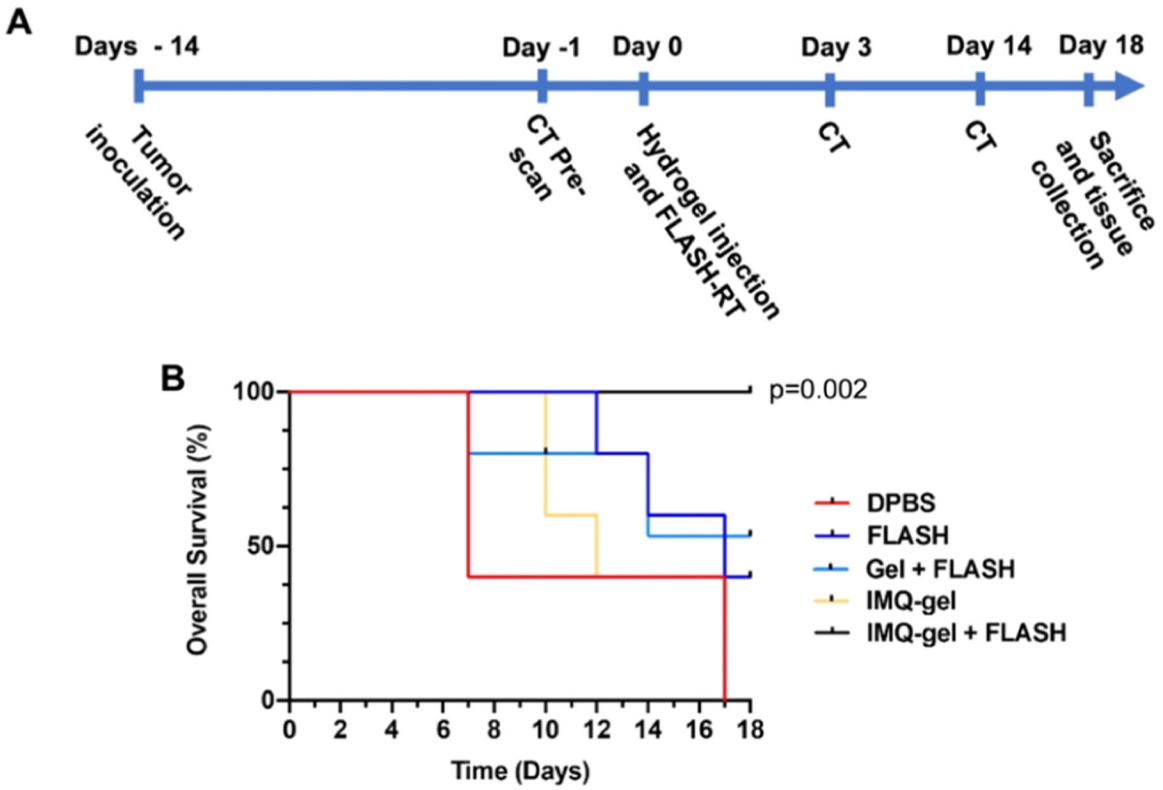

Figure 4.

In vivo evaluation of the tumor growth inhibition effect of the IMQ-loaded hydrogel and FLASH-RT over 18 days. The mice are divided into the following groups: DPBS (vehicle control group), FLASH (FLASH-RT only), Gel + FLASH (AuNP-hydrogel with FLASH-RT), IMQ-gel (AuNP-IMQ-gel), and IMQ-gel + FLASH (AuNP-IMQ-gel with FLASH-RT). (A) Experimental design of the study. (B) Kaplan–Meier curve for the experiment. Statistical comparisons were done with log-rank analysis using Datatab.

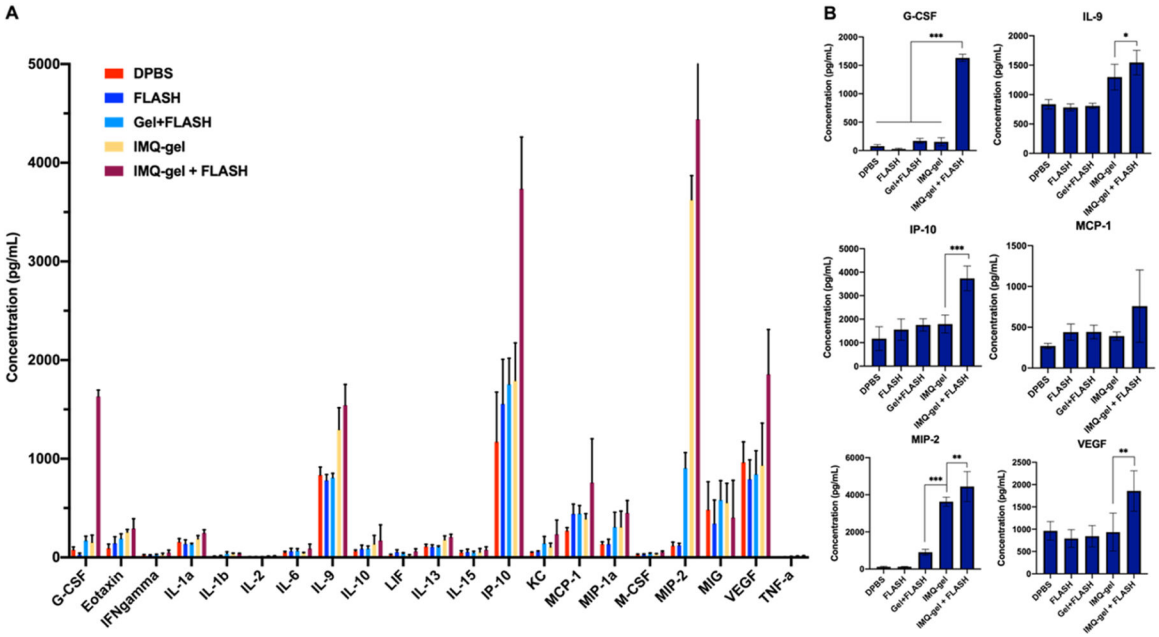

Figure 5.

Luminex multiplex analysis of cytokine levels in B16–F10 tumors 4 days after treatment. A combination of FLASH-RT and IMQ immunotherapy induces cytokine production in the B16–F10 tumors. (A) Cytokine profiles in B16–F10 tumors. (B) Concentrations of G-CSF, IL-9, IP-10, MCP-1, MIP-2, and VEGF in B16–F10 tumors 4 days after treatment.

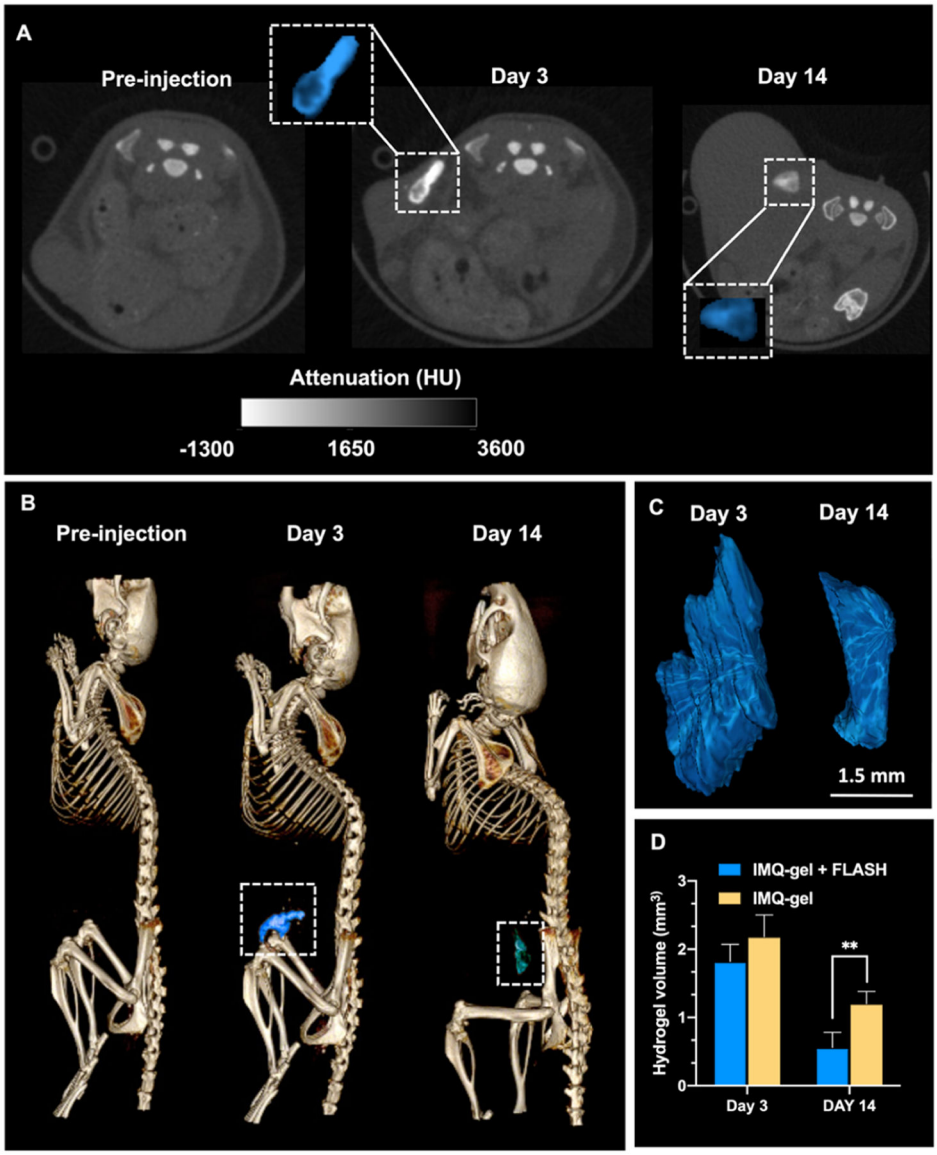

Figure 6.

In vivo images and hydrogel volume analysis. (A) Representative CT images of AuNP-IMQ hydrogel injected in the right flank, at different time points: preinjection, 3 days postinjection, and 14 days postinjection. Insets are enlarged images of injected hydrogels highlighted in blue. (B) Representative 3D CT images of a mouse with the hydrogel highlighted in blue. (C) 3D reconstructions of the hydrogels based on CT images in panel (B). (D) Quantification of the hydrogel degradation by comparing the hydrogel volumes.